JOURNAL OF CATALYSIS 157, 414–422 (1995)

Characterization of Ammonia Adsorption on Ruthenium Sulfide: Identification of Amino Species by Inelastic Neutron Scattering

Hervé Jobic,[1] Michel Lacroix, Thierry Decamp, and Michèle Breysse

Institut de Recherches sur la Catalyse, CNRS, 2 Avenue Albert Einstein, 69626 Villeurbanne Cedex, France

Received February 13, 1995; revised June 7, 1995; accepted July 31, 1995

The interaction of ammonia with the surface of a model ruthenium sulfide catalyst has been investigated using conventional adsorption measurements, temperature programmed desorption and inelastic neutron scattering. This work has provided evidence that the amount and also the nature of adsorbed species vary with the sulfur to metal ratio of the solid. On the unreduced sample, ammonia interacts weakly with the solid and ammonium ions are not observed. On the partially desulfurized catalyst, the chemisorption of ammonia is dissociative. The NH_2 fragment is bonded to a coordinatively unsaturated ruthenium ion formed upon reduction of the solid while the proton is trapped by a sulfur anion leading to the formation of SH groups. It was previously shown that hydrogen adsorption also involves unsaturated sites. Adsorption of ND_3 on a hydrogen-covered surface provokes a desorption of HD indicating that a competition of adsorption occurs between hydrogen and ammonia. This result explains why ammonia generally acts as a poison for hydrogenation, hydrodenitrogenation, and hydrodesulfurization reactions. © 1995 Academic Press, Inc.

INTRODUCTION

It is well established that transition metal sulfides are efficient catalysts for performing several reactions such as hydrodesulfurization, hydrodenitrogenation, and hydrogenation. In the last two decades, extensive studies devoted to the understanding of sulfide catalysts have provided evidence that their catalytic properties are related to the presence of coordinatively unsaturated sites (CUS) formed upon partial reduction of the catalyst surface under the operating conditions required to carry out reaction (1–5). Besides these unsaturated sites, the existence of sulfhydryl groups has been demonstrated by several techniques, including inelastic neutron scattering, ^1H NMR, Raman, and recently Fourier Transform IR spectroscopies (6–8). The formation of such SH entities may arise from the heterolytic adsorption of H_2 on a coordinatively unsaturated site on the metal atom and a neighbor sulfur atom or from the heterolytic adsorption of H_2S which is almost always present in the feed during the determination of the catalytic activity. While agreement on the importance of CUS for developing catalytic properties in all reactions involved in the hydrotreatment processes has been reached, many studies related to the determination of model reaction mechanisms have also assumed that the presence of Brønsted acid sites (SH groups) could be of prime importance (9–17).

Chemisorption of small molecules has been successfully applied for characterizing the surface properties of solids. By probing the interaction of basic molecules with oxide surfaces, information is often obtained on the coordination unsaturation of surface cations, on the acid–base properties of the hydroxyl groups, and on the nature of Lewis or Brønsted acid sites. For this purpose, ammonia and pyridine have been widely utilized because they possess a lone pair of electrons at the nitrogen atom available for donation to surface species and because they can also accept a proton from other species during bonding (18). By analogy with oxides the utilization of such probe molecules has been extended to sulfide catalysts. However, the nature and localization, CUS (Lewis site) or SH, of adsorbed nitrogen-containing molecules is still not completely elucidated. A reasonable way to tackle this fundamental problem of site identification on this kind of catalyst would be to relate both the amount of adsorbed molecules and the catalytic properties to the same criterion of surface characterization. Monitoring the number of CUS may be obtained by progressive desulfurization of the solid by a hydrogen treatment at increasing temperature and contact time. Recently we have studied the interaction of hydrogen with the surface of an unsupported ruthenium sulfide (5, 19–20). This solid has been chosen for its outstanding catalytic properties for hydrodesulfurization and hydrogenation reactions (21, 22). By varying the temperature of reduction between 373 and 573 K it has been shown that about 45% of the total sulfur content can be eliminated from the solid without any noticeable modification of the

[1] To whom correspondence should be addressed. E-mail: jobic@catalyse.univ-lyon1.fr.

0021-9517/95 $12.00
Copyright © 1995 by Academic Press, Inc.
All rights of reproduction in any form reserved.

structural and morphological properties. Accordingly, different reduced states can be obtained at moderate temperature without changing the crystal structure of the initial pyrite phase.

Hydrogen thermodesorption studies performed on different reduced ruthenium sulfide surfaces have shown the presence of two hydrogen species, the concentration of which drastically depended on the degree of reduction of the solid. In agreement with these results, ^1H NMR study of the reduced samples has revealed two signals located at 5.1 and −7.4 ppm, with respect to tetramethylsilane, respectively ascribed to SH groups and to hydride-type adsorbed species (20). More recently, two hydryl species have been observed by inelastic neutron scattering, in addition to the usual sulfhydryl groups (19). Therefore the relative population of Brønsted and Lewis sites changes with the sulfur to metal ratio and consequently variations of the amount and nature of adsorbed nitrogen species could be foreseeable.

The aim of this work was to study the variation in the adsorption of ammonia versus the sulfur to metal ratio of ruthenium sulfide and to characterize the adsorbed species as well as the nature of the adsorbing site. For this purpose, the following techniques were used. Gravimetry was employed for determining the adsorption capacity and inelastic neutron scattering for the identification of adsorbed species. Furthermore, the competitive adsorption between hydrogen and ammonia was studied by means of deuterated ammonia.

EXPERIMENTAL METHODS

Catalyst Preparation

Ruthenium sulfide was prepared by precipitation at room temperature from an aqueous solution of $RuCl_3$ by pure H_2S and by further sulfidation under an H_2S flow at 673 K for 2 h. The catalyst was cooled down to room temperature under the same atmosphere, flushed with an oxygen-free inert gas and stored in a sealed bottle. X-ray diffraction confirmed that the resulting solid has the expected pyrite structure and elemental analysis indicated a sulfur to metal ratio equal to 2.25. From HREM studies the solid may be considered as being formed by a collection of homodispersed spheres having a mean diameter of 45 Å, in agreement with the particle size determined by the broadening of the main x-ray diffraction peaks.

NH_3 Adsorption Measurements

The adsorption capacities of NH_3 were determined gravimetrically in a Sartorius 4433 microbalance working in a dynamic mode. The freshly sulfided sample was transferred into the balance and then submitted to a vacuum pretreatment at 393 K for 15 h. During this desorption procedure it was verified by mass spectroscopy that the catalyst did not lose sulfur. The temperature was then decreased to room temperature and the solid was contacted with hydrogen. The setup was heated to the desired temperature allowing an *in situ* reduction of the catalyst, cooled under the same atmosphere to room temperature, and swept with nitrogen. Adsorption measurements were performed at room temperature by flushing the solid with a mixture containing 75 Torr of diluted ammonia in nitrogen until a stabilized weight was achieved. The irreversible adsorption was determined by replacing the mixture by a pure nitrogen flow. To prevent reaction of H_2S or NH_3 with the electrobalance components a flow of nitrogen was maintained through the balance case in order to avoid back-diffusion of corrosive gases by means of a long and narrow tube carrying N_2 from the balance case to the top of the sample basket.

ND_3 Adsorption Measurements

Adsorption measurements of deuterated ammonia were performed in a dynamic microreactor. This system included a specific UV-photodetector (HNU Photoionization detector equipped with a 10.2-eV UV light source) which allowed an *in situ* reduction. The gas phase composition was determined by means of a mass spectrometer (Fisons Instruments) equipped with a VG quadrupole analyzer using a Faraday detector. A silica capillary tube heated at 453 K bled off continuously a small fraction of the gas phase into the spectrometer. The time response for analyzing 7 masses, H_2, HD, D_2, ND_3, ND_2H, NDH_2, and NH_3, was less than 10 s (no H_2S, HDS, or D_2S was detected during a run). The amount of H_2 and D_2 was determined by calibrating the mass spectrometer with known amounts of each gas. The response factor for HD was calculated by heating the catalyst in the presence of an equimolar mixture of H_2 and D_2 at a temperature which allowed the thermodynamic equilibrium to be attained. Concerning ND_3 and NH_3, it was observed that these molecules cracked inside the ionization chamber with the same fragmentation factor leading respectively to ND_2^* and NH_2^*. Therefore the determination of the relative concentrations of the different NH_xD_y were calculated taking into account the cracking patterns of each species and assuming that the probability of ionization of each species is not affected by the number of hydrogen or deuterium atoms in the molecule. The amount of hydrogen titrated with ND_3 was calculated according to the equation

$$[H_2^t] = \sum_{x=1}^{2} \frac{x}{2}[ND_yH_x] + \frac{1}{2}[HD]. \quad [1]$$

Similarly, the amount of deuterium released is given by

$$[D_2^t] = \frac{1}{2}[HD] + [D_2]. \quad [2]$$

Inelastic Neutron Scattering (INS)

The neutron experiments were performed on the pulsed neutron spallation source ISIS, at the Rutherford Appleton Laboratory (UK), using the time-focused crystal analyzer spectrometer TFXA. This spectrometer is an indirect geometry time-of-flight spectrometer. Pulses of white neutrons illuminate the sample and only those neutrons which excite transitions within the sample, and still retain a final energy of 4 meV, are detected (23). The whole energy transfer range, 20–4000 cm^{-1}, is analyzed simultaneously and data are accumulated until the statistics are reasonable (the time needed to obtain one spectrum is typically 12 h). The individual time-of-flight spectra (detectors) are converted to an energy scale before they are added together. The instrumental resolution $\Delta E/E$ is circa 2% and the precision on the frequencies is ± 10 cm^{-1}.

The powdered samples ($\approx$27 g) were transferred, inside a glove box purged with Ar, into cylindrical vacuum-tight aluminum containers. All the neutron spectra were recorded at 25 K, the neutron cells being placed in a cryostat. The evacuation and loading of the samples were performed out of the cryostat, on an all-metal vacuum line. Ammonia uptake was measured volumetrically. In order to obtain a good contrast between the scattering from the adsorbate and from the catalyst, only the adsorption of NH_3 (i.e., undeuterated ammonia) was studied (hydrogen has the largest incoherent scattering cross section of all atoms).

Computation of the INS Intensities

INS is analogous to Raman scattering spectroscopy, i.e., neutrons exchange energy with a molecular system and excite transitions between vibrational levels. The measured quantity is the double-differential cross section which can be written as (24)

$$\frac{d^2\sigma}{d\Omega\, dE} = \frac{\mathbf{k}}{\mathbf{k}_0} \sum_d \frac{\sigma_d^{\text{inc}}}{4\pi} S_d^{\text{inc}}(\mathbf{Q}, \omega), \qquad [3]$$

where the incident and final wave vectors, $\mathbf{k}_0$ and $\mathbf{k}$, define the neutron momentum transfer Q as $\mathbf{Q} = \mathbf{k} - \mathbf{k}_0$. The sum on d is over the different atoms in the molecule but the scattering from hydrogen atoms dominates because of its large incoherent cross section σ_H^{inc}. The incoherent scattering function, $S_d^{\text{inc}}(\mathbf{Q}, \omega)$, can be calculated for a molecule by resolving molecular vibrations into normal modes. For a sample at low temperature, the following expression can be obtained for a fundamental λ:

$$S_d^{\text{inc}}(\mathbf{Q}, \omega) = \exp(-2W_d) \frac{\hbar |\mathbf{Q} \cdot \mathbf{C}_d^\lambda|^2}{2m_d \omega_\lambda} \delta(\omega - \omega_\lambda). \qquad [4]$$

One obtains a δ function at the frequency ω_λ corresponding to the normal mode λ. Its intensity is governed by the product $|\mathbf{Q} \cdot \mathbf{C}_d^\lambda|^2$, where the vector $\mathbf{C}_d^\lambda$ describes the displacement of the dth atom during the λth normal mode. The Debye–Waller factor, $\exp(-2W_d)$, reflects the dynamical disorder. This factor can also be written $\exp(-Q^2 \langle \mathbf{u}_d^2 \rangle)$, where $\langle \mathbf{u}_d^2 \rangle$ is the mean-square amplitude for atom d. In general, the fundamentals will be the most intense features of the spectra but overtones and combination bands can also be observed. Although this complicates the INS spectra, their intensities can be calculated.

If the sample contains hydrogen atoms, the scattered intensity will be mainly due to these atoms because of the large incoherent cross section, the low mass (m_H) of hydrogen, and the fact that hydrogen atoms often have the largest displacement vectors during the normal modes. For hydrogen bonded to heavy atoms (like H with Ru), the heavy atoms can be considered as fixed during the local modes of hydrogen. Therefore, the modulus of the displacement vector for an adsorbed hydrogen atom during any vibration will be close to unity.

On the other hand, for a molecular system, one has to compute the displacement vectors for all atoms during each vibration. These vectors can be derived from a force field calculation, which also yields the frequencies ω_λ, the displacement vectors $\mathbf{C}_d^\lambda$, and the mean-square amplitudes $\langle \mathbf{u}_d^2 \rangle$.

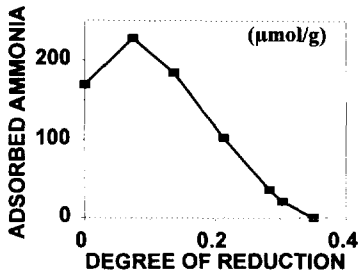

FIG. 1. Gravimetric adsorption of NH_3. Irreversible amount of adsorbed ammonia versus the degree of reduction (α) of the solid.

RESULTS

Gravimetric Adsorption of NH_3

Gravimetric experiments were made on samples which had been subjected to various degrees of reduction (α), where α is the ratio of the amount of H_2S evolved to the total sulfur content. The results showed that the interaction of ammonia with the solid exhibits an important reversible uptake which represents circa 400 μmol/g. This reversible fraction is rather independent of the degree of reduction of the catalyst suggesting that it is related to weakly bonded species. The curve giving the irreversible part of the adsorption presented in Fig. 1 shows an initial adsorption of

TABLE 1

Composition of Samples A, B, and C

Sample	Temperature of pretreatment (K)	Degree of reduction (α)[a]	Amount of H_2 (μmol/g)	Composition
A	Unreduced	0	120[b]	$RuS_{2.25}H_{0.04}$
B	373	0.13	485	$RuS_{1.96}H_{0.17}$
C	523	0.27	155	$RuS_{1.64}H_{0.05}$

[a] α is the ratio of the amount of H_2S evolved to the total sulfur content.
[b] Desorbs as H_2S.

about 170 μmol/g. This amount slightly increases at the beginning of the reduction and then linearly falls and becomes almost undetectable for a reduction state of about 35%. As mentioned in the Introduction, as far as α does not exceed 0.45 the textural and structural properties of the catalysts are identical to those of the nonreduced state (5). Thus it appears that the decrease in the amount of chemisorbed ammonia cannot be ascribed to a sintering of the active phase. As the amount of adsorbed ammonia mostly decreases with sulfur removal, it seems likely that its adsorption requires a sulfur species. This technique, being based only on weight changes, does not allow the measurement of hydrogen and ammonia competitive adsorption so that experiments with deuterated ammonia were performed using a mass spectrometer.

Interaction of ND_3 with RuS_2 at Various Reduction States

Three samples were selected for this study: the nonreduced solid denoted sample A, a solid slightly reduced (α = 0.13) sample B, and a more reduced solid, sample C, which chemisorbs a smaller amount of ammonia. The composition of these three samples is reported in Table 1.

Sample A. The catalyst was transferred into the reactor, degassed at 423 K under a nitrogen flow and then the reactor was switched off and a ND_3 flow was established into the unit until stabilization of the signal coming out from the mass spectrometer was achieved. Figure 2a shows the results obtained when the reactor was opened. The signal related to mass 20 (ND_3) decreased due to the purge of the reactor and to the adsorption process. Neither hydrogenated compounds NH_xD_y (Fig. 2a) nor H_2, HD, and D_2 were detected on such a catalyst. The amount of ND_3 reversibly adsorbed was then eliminated by flushing the solid with an inert gas and the irreversible fraction fixed on the catalyst surface was determined by heating the sample to 573 K. Figure 2b indicates that only ND_3 desorbed at a temperature of about 373 K. The amount of ND_3 adsorbed, calculated by integrating the evolution of the signal against time, corresponds to 160 ± 20 μmol/g, in agreement with the value previously observed by TGA.

Samples B and C. Figure 3 reports the results obtained on sample B. The data clearly indicate that when ammonia was contacted with the reduced solid there was an exchange reaction with chemisorbed hydrogen leading to the formation of NH_xD_y species (Fig. 3a). Simultaneously, the interaction of ND_3 with the catalyst provokes a desorption of HD suggesting a competition of adsorption between

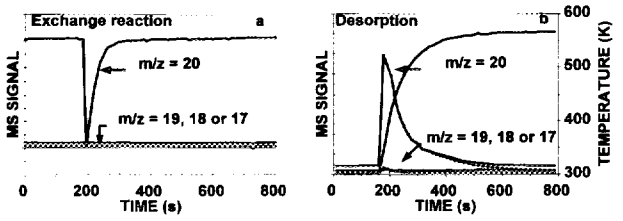

FIG. 2. Interaction of deuterated ammonia with the nonreduced solid (sample A). (a) Variation of the MS signals with time. (b) Thermodesorption of adsorbed ammonia species.

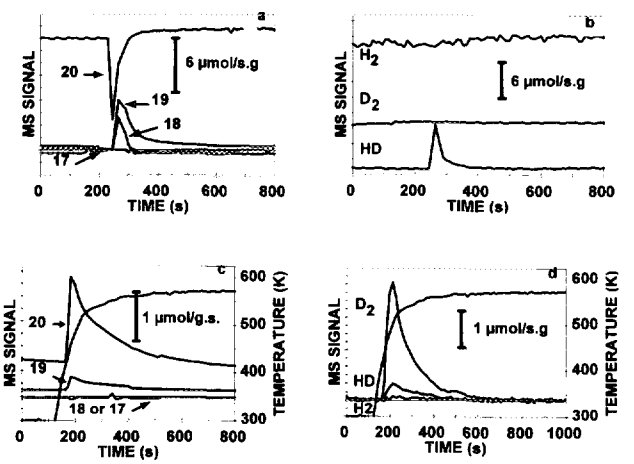

FIG. 3. Interaction of deuterated ammonia with the 13% reduced solid (sample B). (a) Variation of the NH_xD_y MS signals with time. (b) Variation of the H_xD_y MS signals with time. (c) Thermodesorption of adsorbed NH_xD_y species. (d) Thermodesorption of adsorbed H_xD_y species.

TABLE 2

Amount of NH_xD_y and H_xD_y (Expressed in μmol/g) Observed during both Exchange Reaction and Thermodesorption

Sample	Experiment	ND_3 (μmol/g)	ND_2H (μmol/g)	NDH_2 (μmol/g)	HD (μmol/g)	D_2 (μmol/g)
B	Exchange reaction		430	135	170	0
	Desorption	185	40	0	44	365
C	Exchange reaction		100	51	50	0
	Desorption	43	4		10	120

ammonia and hydrogen (Fig. 3b). Figures 3c and 3d show that during desorption mostly ND_3 and D_2 are released from the catalyst surface. With respect to the results obtained on sample A, the maximum desorption temperature of ND_3 is shifted to a higher temperature suggesting a more strongly adsorbing state. Similar results were observed over sample C (α = 27%).

Mass balances of the different species detected during both exchange and desorption experiments are summarized in Table 2. According to these data, samples B and C adsorb respectively 225 and 47 μmol of ammonia per gram of catalyst. Moreover, the amounts of hydrogen and deuterium either titrated with ND_3 or evolved as HD and desorbed as D_2 (calculated from Eq. [1] and [2]) are identical, i.e., 477 and 472 μmol/g, respectively, for sample B, and correspond to the total amount of hydrogen initially present at the surface of this reduced sample (compare with Table 1). This result demonstrates that all the hydrogen species fixed on the solid during the reduction process react with deuterated ammonia.

As stated in the Introduction, two kinds of hydrogen are retained by the catalysts after a reductive treatment. Indeed, Fig. 4 shows that on samples B and C the TPD patterns can be decomposed into two peaks: there is a low-temperature one centered at circa 400 K and a high-temperature peak at about 480 K. As mentioned above all these hydrogen species are replaced by deuterium by exchange with deuterated ammonia and a fraction of them compete with the nitrogen-containing molecule leading to the desorption of HD. Interestingly, the comparison of the H_2 and D_2 TPD profiles provides evidence that only the high temperature peak remains after the exchange reaction, indicating that ammonia interacts with the same sites as those responsible for the adsorption of weakly bonded hydrogen.

In order to check whether the ammonia adsorption capacity can be affected by the presence of preadsorbed hydrogen, a second experiment was performed on a solid from which hydrogen was removed prior to ammonia adsorption. Figure 5 shows the results obtained. As expected, the formation of hydrogenated ND_3 and the desorption of HD were not detected. Moreover, both the TPD profile and the amount of adsorbed ammonia were found to be identical with the data obtained in the presence of adsorbed hydrogen (210 μmol/g for sample B).

Inelastic Neutron Scattering

Due to the large mass of catalyst used for the INS measurement, sample B was treated under H_2 at a higher tem-

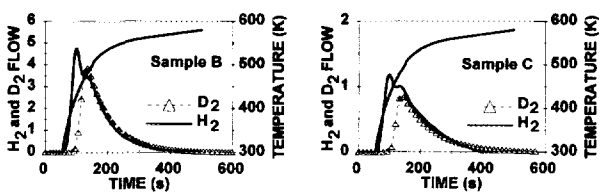

FIG. 4. Thermodesorption of the H_xD_y species adsorbed on samples B (α = 0.13) and C (α = 0.27) before contacting the catalysts with ND_3 (bold lines) and after contacting the catalysts with ND_3 (triangles). Flows are expressed in μmol s^{-1} g^{-1}.

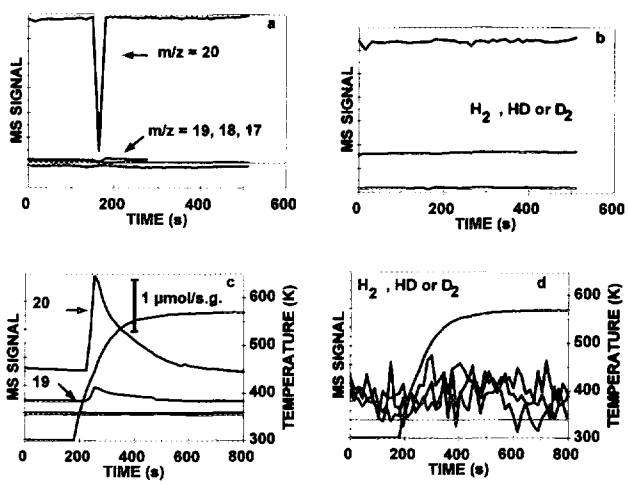

FIG. 5. Interaction of deuterated ammonia with the 13% reduced and hydrogen desorbed solid (sample B). (a) Variation of the NH_xD_y MS signals with time. (b) Variation of the H_xD_y MS signals with time. (c) Thermodesorption of adsorbed NH_xD_y species. (d) Thermodesorption of adsorbed H_xD_y species.

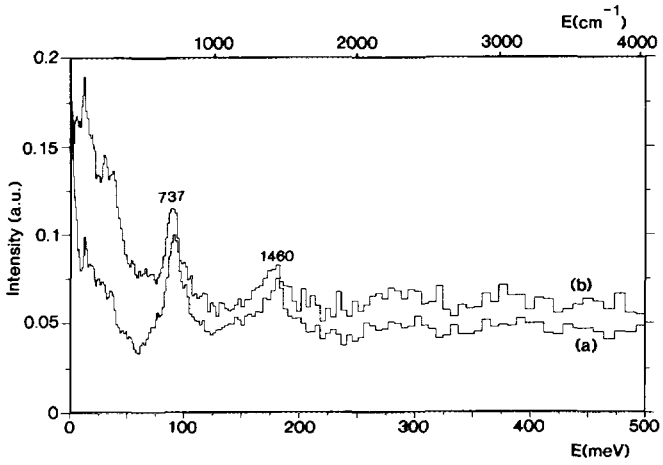

FIG. 6. Inelastic neutron scattering spectra of sample A (peak frequencies are in cm^{-1}). (a) Bare catalyst. (b) After contacting the catalyst with NH_3.

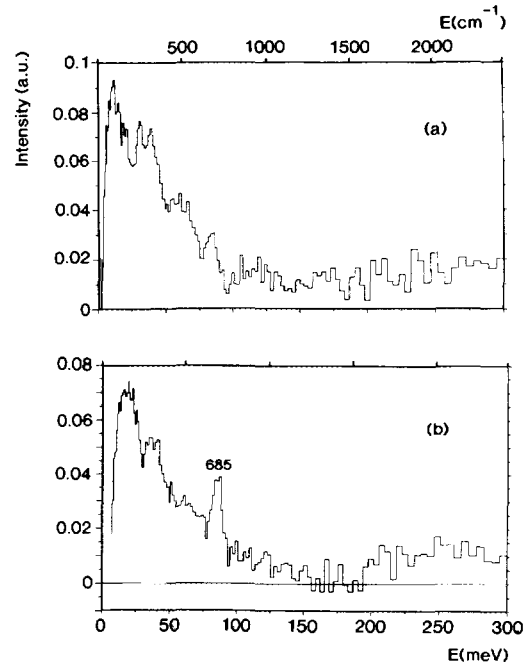

FIG. 7. Inelastic neutron scattering spectra of sample A obtained after subtracting the signal of the bare catalyst (peak frequencies are in cm^{-1}). (a) Spectrum obtained after adsorption at room temperature. (b) Spectrum obtained after heating the cell at 600 K.

perature (513 K) than during the TPD experiment to obtain the same degree of reduction. Samples A and B were studied with this technique. NH_3 was introduced onto the samples at room temperature, eliminated in various conditions, but the INS spectra were all recorded at 25 K.

The INS spectrum of degassed sample A was first recorded; the spectrum is shown in Fig. 6a. Several bands can be measured below 400 cm^{-1}: they correspond to hydrogen-coupled lattice vibrations. The peak at 737 cm^{-1} is assigned to SH bending modes, the first harmonic being observed at 1460 cm^{-1}. The cell was then taken out of the cryostat and NH_3 was introduced at room temperature. The final pressure was 100 mbar and the sample was left for 24 h to equilibrate. The adsorbed volume was 3.9 cm^3 g^{-1} (170 μmol/g). Then, the gas phase was eliminated until the pressure in the cell was less than 1 mbar. During the evacuation, weakly adsorbed ammonia was also removed. The sample was cooled to 25 K and the INS spectrum was again recorded (Fig. 6b). The difference spectrum is given in Fig. 7a. After heating the sample at 600 K in the closed cell and evacuation of the gas phase, the INS spectrum shown in Fig. 7b was obtained. The main differences with the results obtained at room temperature are a decrease of the overall intensity and the development of a peak at 685 cm^{-1}.

In order to study possible interactions of ammonia with sulfhydryl or hydryl species evidenced on the reduced catalyst (19), the adsorption of ammonia on sample B partly covered with hydrogen was followed by INS. The spectrum of sample B, onto which hydrogen was adsorbed with a pressure of 1 mbar, is reported in Fig. 8a. The broad band at 683 cm^{-1} is due to SH bending modes and the peaks at 542 and 826 cm^{-1} are due to RuH bending modes (19). During the adsorption of ammonia at room temperature, a small pressure rise was observed which could be interpreted as hydrogen desorption from the coordinatively unsaturated sites. This made the determination of the adsorbed ammonia quantity less reliable (from the final pressure in the line, the adsorbed volume is about 5.1 cm^3 g^{-1} or 228 μmol/g). A pressure of 100 mbar was left in the neutron cell and after cooling to 25 K the INS spectrum

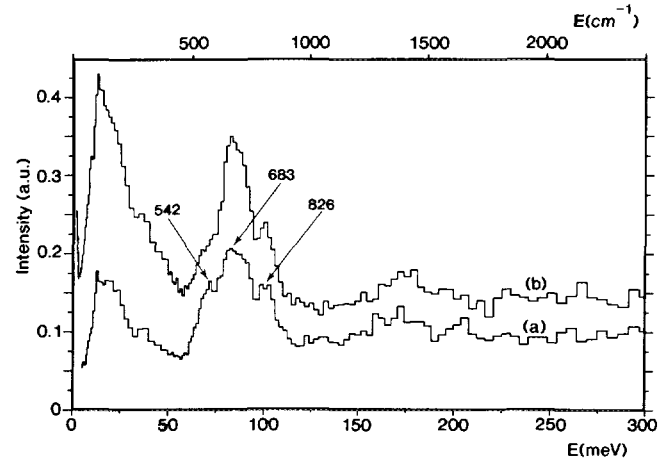

FIG. 8. Inelastic neutron scattering spectra of the 13% reduced solid (sample B). (a) Spectrum of the hydrogen-covered surface. (b) Spectrum of the hydrogen-covered surface with ammonia.

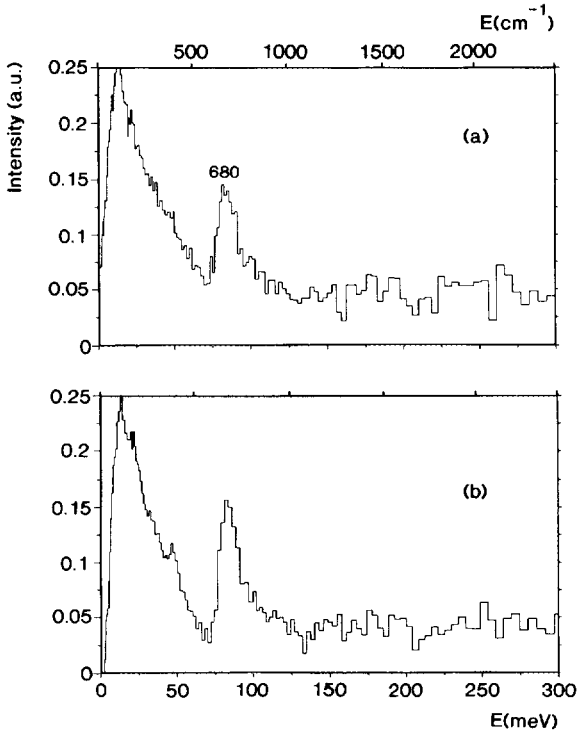

FIG. 9. Inelastic neutron scattering spectra of the 13% reduced solid (sample B). (a) Difference spectrum (Fig. 8b–Fig. 8a). (b) Difference spectrum after evacuation of the cell at room temperature.

shown in Fig. 8b was obtained. It appears that the intensity at 683 cm^{-1}, which is due to SH groups, has increased. This becomes more obvious in the difference spectrum which is given in Fig. 9a. By comparing the peak intensities in Figs. 7a and 9a, one can estimate that the quantity of ammonia adsorbed on the reduced catalyst is about twice the quantity left on the unreduced sample. After pumping to 10^{-2} mbar on sample B at room temperature, the INS spectrum shown in Fig. 9b after subtraction of the bare catalyst contribution was obtained. This pumping only removed physisorbed hydrogen and hydrogen weakly adsorbed on the CUS. This can be deduced from the decrease of the baseline and from the more pronounced gap at 550 cm^{-1} due to elimination of one hydryl species, as already reported in Ref. (19).

DISCUSSION

The low-temperature method used for the synthesis of bulk ruthenium sulfide leads to a homogeneous solid, the composition of which corresponds to $RuS_{2.25}H_{0.04}$. For small crystallites (45 Å), the stoichiometric RuS_2 phase should contain some anionic vacancies which could accommodate extra sulfur during sample preparation since the solid was sulfided with H_2S at 673 K and cooled to room temperature in the presence of the sulfiding gas. This excess of sulfur is however weakly bonded to the catalyst surface since a mild hydrogen treatment at a temperature as low as 373 K provokes its elimination. Although the nature of this extra sulfur is not completely elucidated its presence has also been observed on molybdenum sulfide (25). For RuS_2, a fraction of this species exists as SH groups because H_2S is formed only by gently heating sample A under a nitrogen flow. Furthermore, the existence of such sulfhydryl groups is also consistent with the presence of the band observed at 737 cm^{-1} by INS. Previous TPR work performed on a series of supported or unsupported ruthenium sulfide particles have provided evidence for three different kinds of sulfur species whose relative concentrations depend on the crystallite size of the sulfided phase (26). The use of a geometrical model similar to the one developed by Kasztelan (27) for molybdenum sulfide has allowed us to estimate the amount of sulfur bonded to surface ruthenium atoms. According to this model, and taking into account the average particle size of the sample, the calculated S/Ru ratio at the surface is close to 3. Therefore, the surface of sample A could be considered as completely covered by sulfur species (Scheme 1).

According to the gravimetric study reported in Fig. 1, sample A adsorbs a noticeable amount of ammonia (170 μmol/g). From TPD experiments ammonia seems to be weakly bonded since the adsorbed species are released from the surface at a temperature as low as 373 K. The loosely bonded character between ammonia and sample A was also observed by INS. As a matter of fact, the spectrum obtained after adsorption of NH_3 at room temperature, Fig. 7a, contains several peaks below 800 cm^{-1} assigned to hindered translations and rotations of weakly bonded ammonia. Such features have also been observed in two-dimensional metal–ammonia solid solutions formed by high-stage caesium graphite intercalates (28). The INS spectrum does not indicate the presence of ammonium ions since in this case N—H bending modes would be expected near 1450 and 1700 cm^{-1}; such modes have been reported in NH_4Y zeolites (29). After heating at 600 K, some decomposition of ammonia occurs on sample A, as shown by the appearance of the peak at 685 cm^{-1}. During this thermal treatment, the catalyst has been partially reduced since the SH bending modes are measured at the same frequency as on the reduced sample. This shows that

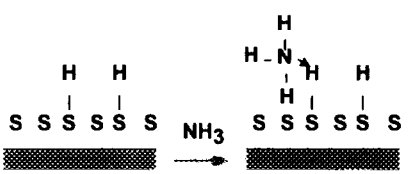

SCHEME 1

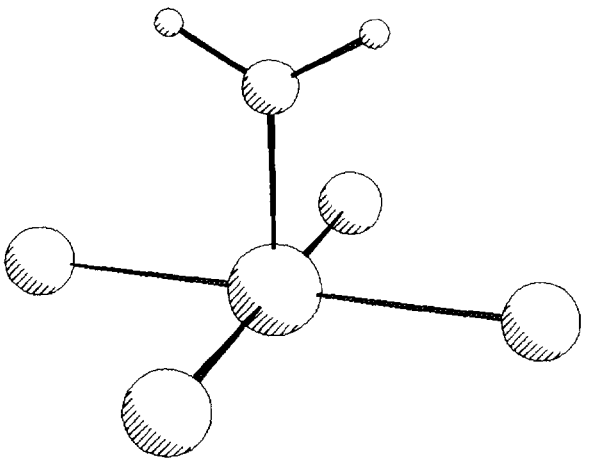

FIG. 10. Adsorption geometry of the NH_2 fragment on the RuS_2 surface.

ammonia reacts with the sulfide surface at high temperature, as suggested from TPD experiments on supported NiMo catalysts (30). At room temperature, the lack of strong interaction between ammonia and sample A is probably related to hydrogen bonding from the nitrogen atom to some remaining SH groups or via a hydrogen atom with a surface sulfur ion.

Upon reduction, the solid contains both SH groups and anionic vacancies partly occupied by hydrogen ligands (Ru—H) giving rise to bending modes at 683 cm^{-1} (for SH) and at 542 and 826 cm^{-1} for the hydryl species. With respect to sample A the SH bands are shifted to lower frequencies which indicates an increase of Brønsted acidity. As for the unreduced catalyst, there is also no indication of formation of ammonium ions since the N—H bending modes are not observed. This result suggests that the Brønsted acidity of unsupported ruthenium sulfide is not strong enough to lead to the formation of ammonium ions. This observation is in agreement with previous catalytic results obtained in model reactions characteristic of C—N and C—C bond cleavages (15) which showed that this sulfide presents very poor acidic properties.

The INS spectra show that ammonia is decomposed on sample B leading to the formation of amino (NH_2) and SH groups. The broad band with a maximum at 100 cm^{-1} contains six modes due to the hindered translations and rotations of the amine groups, while the peak at 680 cm^{-1} corresponds to two SH bending modes which appear to be almost degenerate. In order to test this assignment, a simulation of the INS spectrum presented in Fig. 9b was made. Two different species were considered: (i) a hydrogen atom bonded to one sulfur atom and having two bending modes at 653 and 702 cm^{-1}, and (ii) a NH_2 group weakly bonded to a Ru atom (Fig. 10). The calculations were made using expressions [3] and [4]. For the amine species the intensities from overtones and combinations were also computed. The effect of the Debye–Waller factor, $\exp(-Q^2\langle \mathbf{u}_d^2\rangle)$, was neglected because of the small values of the product $Q^2\langle \mathbf{u}^2\rangle$: the vibrations of the amine group occur at low energy transfers where Q^2 is small and for the H atoms bonded to S atoms, the mean-square amplitude is small (on the spectrometer TFXA, Q^2 is proportional to the energy transfer). At higher energy transfers, which imply larger Q^2 values, the effect of the Debye–Waller factor is much more pronounced. For example, no intensity is left at the frequency of the fundamentals of the NH_2 bending or NH stretches; all the intensity goes to multiphonon features. The calculated spectrum is compared in Fig. 11 with the experimental spectrum in the range 20 to 800 cm^{-1}. The agreement between the two spectra is reasonable and this supports the assignment of the INS spectra in terms of amine and sulfhydryl groups. It can be noted that NH_2 groups have also been identified during the adsorption of ammonia on oxides, e.g., Ref. (31), on nitrides (32), and on transition metal surfaces (33).

Besides the formation of SH groups, the TPD and INS experiments indicate that hydrogen is also bonded to a coordinatively unsaturated ruthenium cation. The interaction of ND_3 with this hydrogen-covered surface leads to an exchange reaction involving both hydrogen species.

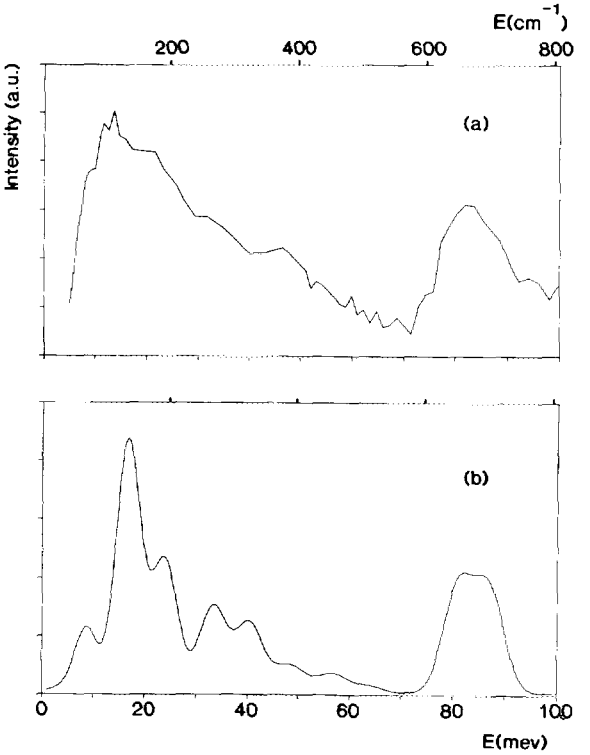

FIG. 11. Inelastic neutron scattering spectra obtained for sample B: (a) experimental (spectrum range 20 to 800 cm^{-1}) and (b) calculated from the contributions of NH_2 and SH species.

However, if we look at the adsorption process, ammonia competes only with the hydryl entities according to the overall reaction

$$Ru-H + ND_3 \rightarrow Ru-ND_2 + HD,$$

with $[HD] = \frac{1}{2}[H_2]_{Ru-H}$.

As a matter of fact, the amount of adsorbed ND_3 molecules is twice the amount of hydryl species retained by the solid upon reduction. As this form of adsorbed hydrogen was found to be the active species for hydrogenation reactions (5), this result explains why nitrogen-containing molecules act as a poison for this reaction.

Over reduced but hydrogen free surfaces, the amount of adsorbed ammonia is the same as over hydrogenated surfaces. This result can be explained if we assume that the product proton has the mobility and the reactivity required to move from the dissociative site to a sulfur atom forming a SH group. If the surface is sulfur depleted, i.e., for reduction states higher than 0.45, no adsorption occurs because the proton cannot be stabilized or because the electronic properties of the adsorbing sites are modified.

CONCLUSIONS

The combined use of three techniques, i.e., gravimetry, inelastic neutron scattering, and ND_3 exchange, has allowed us to elucidate the interaction between ammonia and ruthenium sulfide. Ammonia is adsorbed dissociatively into a proton and an amino group. The proton is fixed on a sulfur anion and the amine fragment on a coordinatively unsaturated ruthenium ion. Taking into account the fact that hydrogen is adsorbed on the same sites, a competitive adsorption between the two molecules is observed which explains why ammonia inhibits hydrotreating reactions. The ammonium ion is never observed whatever the sulfidation state of the solid. This study shows that the utilization of ammonia for numbering sites is not reliable.

REFERENCES

1. Tanaka, K., *Adv. Catal.* **33,** 99 (1985).
2. Wambeke, A., Jalowiecki, L., Kasztelan, S., Grimblot, J., and Bonnelle, J. P., *J. Catal.* **109,** 320 (1989).
3. Topsøe, H., Candia, R., Topsøe, N. Y., and Clausen, B. S., *Bull. Soc. Chim. Belg.* **93,** 783 (1984).
4. Nørskov, J. K., Clausen, B. S., and Topsøe, H., *Catal. Lett.* **13,** 1 (1992).
5. Lacroix, M., Mirodatos, M., Breysse, M., and Yuan, S., *in* "Proceedings, 10th International Congress on Catalysis, Budapest, 1992" (L. Guczi, F. Solymosi, and P. Tétényi, Eds.), p. 597. Akadémia Kiado, Budapest, 1993.
6. Wright, C. J., Fraser, D., Moyes, R. B., and Wells, P. B., *Appl. Catal.* **1,** 49 (1981).
7. Polz, J., Zeilinger, H., Müller, B., Knözinger, H., *J. Catal.* **120,** 28 (1989).
8. Topsøe, N. Y., and Topsøe, H., *J. Catal.* **139,** 641 (1993).
9. Maternova, J., *Appl. Catal.* **6,** 61 (1982).
10. Muralidhar, G., Massoth, F. E., and Shabtai, J., *J. Catal.* **85,** 44 (1984).
11. Calais, C., Lacroix, M., Geantet, C., and Breysse, M., *J. Catal.* **144,** 160 (1993).
12. Markel, E. J., Schrader, G. L., Sauer, N. N., and Angelici, R. J., *J. Catal.* **116,** 11 (1989).
13. Sutarno, O., Knop, O., and Reid, K. I. G., *Can. J. Chem.* **45,** 1391 (1967).
14. Portefaix, J. L., Cattenot, M., Guerriche, M., and Breysse, M., *Catal. Lett.* **9,** 127 (1991).
15. Breysse, M., Afonso, J., Lacroix, M., Portefaix, J. L., and Vrinat, M., *Bull. Soc. Chim. Belg.* **100 (11–12),** 923 (1991).
16. Lombardo, E., Lo Jacono, M., and Hall, W. K., *J. Catal.* **64,** 150 (1980).
17. Cowley, S. W., and Massoth, F. E., *J. Catal.* **51,** 291 (1978).
18. Kung, M. C., and Kung, H. H., *Catal. Rev.-Sci. Eng.* **27(3),** 425 (1985).
19. Jobic, H., Clugnet, G., Lacroix, M., Yuan, S., Mirodatos, C., and Breysse, M., *J. Am. Chem. Soc.* **115,** 3654 (1993).
20. Lacroix, M., Yuan, S., Breysse, M., Dorémieux-Morin, C., and Fraissard, J., *J. Catal.* **138,** 409 (1992).
21. Pecoraro, T. A., and Chianelli, R. R., *J. Catal.* **67,** 430 (1981).
22. Lacroix, M., Boutarfa, N., Guillard, C., Vrinat, M., and Breysse, M., *J. Catal.* **120,** 473 (1989).
23. Penfold, J., and Tomkinson, J., Rutherford Appleton Laboratory Report, RAL-86-019, 1986.
24. Jobic, H., *in* "Catalyst Characterization" (B. Imelik and J. C. Védrine, Eds.), p. 347. Plenum, New York, 1994.
25. Scheffer, B., Dekker, N. J. J., Mangnus, P. J., and Moulijn, J. A., *J. Catal.* **121,** 31 (1990).
26. Geantet, C., Calais, C., and Lacroix, M., *C. R. Acad. Sci. Ser. 2* **315,** 439 (1992).
27. Kasztelan, S., *C. R. Acad. Sci. Ser. 2* **307,** 391 (1988).
28. Carlile, C., Jamie, I., McL., White, J. W., Prager, M. J., and Stead, W., *J. Chem. Soc. Faraday Trans.* **87,** 73 (1991).
29. Jacobs, W. P. J. H., van Santen, R. A., and Jobic, H., *J. Chem. Soc. Faraday Trans.* **90,** 1191 (1994).
30. Zeuthen, P., Blom, P., Muegge, B., and Massoth, F. E., *Appl. Catal.* **68,** 117 (1991).
31. Coluccia, S., Garrone, E., and Borello, E., *J. Chem. Soc. Faraday Trans 1* **79,** 607 (1983).
32. Haddix, G. W., Jones, D. H., Reimer, J. A., and Bell, A. T., *J. Catal.* **112,** 556 (1988).
33. Bassignana, I. C., Wagemann, K., Küppers, J., and Ertl, G., *Surf. Sci.* **175,** 22 (1986).